

Enhanced Chemotherapeutic Efficacy of PLGA-Encapsulated Epigallocatechin Gallate (EGCG) Against Human Lung Cancer

This article was published in the following Dove Press journal:
International Journal of Nanomedicine

Lingyu Zhang^{1,*}
Wenshu Chen^{1,2,*}
Guihui Tu¹
Xingyong Chen^{1,2}
Youguang Lu³
Lixian Wu¹
Dali Zheng^{1,3}

¹School of Pharmacy, Fujian Medical University, University Town, Fuzhou 350122, People's Republic of China; ²Shengli Clinical College, Fujian Medical University, Fuzhou 350001, People's Republic of China; ³Key Laboratory of Stomatology of Fujian Province, School and Hospital of Stomatology, Fujian Medical University, Fuzhou, 350004, People's Republic of China

*These authors contributed equally to this work

Purpose: Currently, the clinical benefits of tea polyphenols have contributed to the development of efficient systemic delivery systems with adequate bioavailability and stability. In this study, we aimed to establish a nanoparticle model to overcome the shortcomings of epigallocatechin gallate (EGCG) in the treatment of lung cancer.

Materials and Methods: Poly(lactic-co-glycolic acid) (PLGA) nanoparticles (NPs) loaded with EGCG were prepared by the oil-in-water emulsion solvent evaporation technique. The characteristics of NPs, entrapment efficiency, and in vitro release were systematically evaluated. The cellular uptake, cytotoxic activity, and the effect of the formulation on cellular apoptosis of free EGCG and the NPs were compared. The interaction between protein-NF- κ B and EGCG was detected by bio-layer interferometry (BLI). NF- κ B signaling was evaluated by Western blotting and q-RT-PCR. The efficacy of the optimized nanoformulation was evaluated using a patient-derived tumor xenograft (PDX) model.

Results: EGCG-loaded NPs (175.8 \pm 3.8 nm in size) demonstrated its optimal efficacy, with approximately 86.0% of encapsulation efficiency and 14.2% of loading efficiency. Additionally, EGCG-encapsulated PLGA-NPs offered a 3-4-fold dose advantage compared to free EGCG in terms of exerting antiproliferative effects and inducing apoptosis at lower doses (12.5, 25 μ M). Molecular interaction assays demonstrated that EGCG binds to NF- κ B with high affinity ($K_D=4.8\times 10^{-5}$ M). EGCG-NPs were more effective at inhibiting NF- κ B activation and suppressing the expression of NF- κ B-regulated genes than free EGCG. Furthermore, EGCG-NPs showed superior anticancer activity in the PDX model than free EGCG.

Conclusion: These findings indicated that the prepared EGCG-NPs were more effective than free EGCG in inhibiting lung cancer tumors in the PDX model.

Keywords: anticancer, tea polyphenol, nanoparticles, NF- κ B

Correspondence: Dali Zheng
Key Laboratory of Stomatology of Fujian Province, Hospital of Stomatology, Fujian Medical University, 88 Jiaotong Road, Fuzhou 350004, People's Republic of China
Email dalizheng@fjmu.edu.cn

Lixian Wu
School of Pharmacy, Fujian Medical University, 1 Xueyuan Road, University Town, Fuzhou 350122, People's Republic of China
Email 18259000966@126.com

Introduction

Non-small cell lung cancer (NSCLC) comprises about 85% of all diagnosed lung malignancies.¹ Many lung cancer patients are diagnosed at later stages of the disease, leading to a 5-year survival rate of only ~15%.² Chemotherapy and radiation therapy, as well as a combination of both, are used for an attempt to reduce tumor mass and halt disease progression. However, chemotherapeutic agents damage healthy tissues, leading to systemic toxicity and adverse effects. Additionally, they greatly limit the maximum tolerated dose of anticancer drugs which restricts their therapeutic efficacy.³

Phytochemicals that induce fewer side effects have emerged as newer options and effective chemotherapeutics for recalcitrant cancers.^{4,5} (-)-Epigallocatechin-3-gallate (EGCG), an active ingredient in green tea, has been known to effectively inhibit the formation and development of tumors including lung cancer.^{5–10} EGCG may induce cell apoptosis and contribute to lung tumor regression by downregulating the expression of NF- κ B in lung cancer. On the other hand, our previous study also showed that that downregulation of NF- κ B expression is correlated with the anti-proliferative effects of EGCG in A549 and H1299 cells.^{6,7} In spite of promising preclinical findings, the applicability of tea in human cancer therapy is limited owing to a lack of efficient systemic delivery, bioavailability, and stability.¹¹ Notably, previous studies have shown that EGCG inhibited the growth of many cancers, including lung, bladder, and colorectal cancer, with an IC₅₀ more than 100 μ M for 48 h.^{6,12–14}

Furthermore, the excessive uptake of EGCG has been known to cause several adverse effects in the human body, including hepatitis.¹³ Based on these findings, taking EGCG as an anti-tumorigenic agent in clinics should ponder how to deliver EGCG to the right target site and to maintain an appropriate cell fluid level. The establishment of superior EGCG pharmacodynamics and pharmacokinetics in cancer therapy has been a challenging issue.¹²

Nanoparticles (NPs) as drug carriers have drawn considerable attention since NPs possess unique physical properties, such as higher tissue permeability, colloidal stability, and drug bioavailability, as well as relatively lower cost.^{15–17} It has been reported that many different nanosystems have designed to encapsulate EGCG such as EGCG-CS-NPs, EGCG- β -Lg-NPs, EGCG-Au-NPs, EGCG-PLGA-NPs and so on.^{18–21} And these are effective techniques to improve the stability and bioavailability of EGCG. However, compared to EGCG-Au-NPs, the preparation process of EGCG-PLGA-NPs is simple and more economical. In addition, EGCG-PLGA-NPs have better antioxidant effects than EGCG-CS NPs.^{18–21} Polymer-drug conjugates, firstly developed in the mid-1970s, have laid the foundation for new types of anticancer therapeutics.²² Among them, poly(lactic-co-glycolic acid) (PLGA) is an FDA-approved polymer with great biocompatibility and biodegradability. Many researches have demonstrated the great potential of PLGA as a carrier for cancer treatment which has a sphericity is better than β -Lg-NPs.^{22–24}

Here, we established a PLGA drug development model for loading EGCG in a PLGA carrier to enhance uptake, retention, and cytotoxicity in cancer cells in vitro. Additionally, the

antitumor efficacy of the formulated EGCG-NPs was assessed in a patient-derived tumor xenograft (PDX) model. EGCG-NPs demonstrated a significant improvement in lung cancer treatment compared to free EGCG.

Materials and Methods

Cell Culture

The lung cancer cell lines A549 and H1299 were obtained from Chinese Academy of Sciences. Briefly, A549 and H1299 cells were cultured in RPMI-1640 (Thermo Fisher Scientific Inc, Waltham, MA, USA) containing 10% (v/v) fetal bovine serum (Welgene, Inc, Daegu, South Korea) and 50 U/mL penicillin/streptomycin (NCM Biotech, Suzhou, China) at 37°C in 5% CO₂ humidified incubator.

Materials

COOH-terminated PLGA (inherent viscosity range 0.15–0.25 dL/g, lactide/glycolide ratio 50:50, average molecular weight 15,000–24,000), polyvinyl alcohol (PVA, average molecular weight 20,000–30,000) and dichloromethane (DCM) were purchased from Sigma-Aldrich (St Louis, MO, USA). Cell Counting Kit-8 (CCK8), EGCG, and Neil Red were purchased from Dalian Meilun Biotech. The type of water used is ddH₂O.

Preparation of EGCG-Loaded PLGA-NPs

PLGA nanoparticles were prepared using the oil-in-water emulsion solvent evaporation technique PLGA-NPs loaded EGCG. Briefly, for the preparation of EGCG-encapsulated PLGA-NPs, the ratio between the volume of EGCG to the volume of PLGA was 1:20. EGCG (10 mg) was dissolved in deionized water (1 mL) and emulsified with a solution of PLGA (10 mg) dissolved in dichloromethane (1 mL) to form an oil-in-water emulsion. The emulsification was performed using a microtip probe sonicator (Sonics & Materials Inc, Newtown, CT, USA) with a sonicator operated at 200 W over an ice bath. The formed o/w emulsion was poured into 2 mL of a PVA aqueous solution (5%, w/v). The mixture was emulsified for 4 min with a sonicator operated at 200 W. To allow the formation of NPs, the emulsion was stirred for 4 h on a magnetic stir plate at room temperature. NPs were recovered by centrifugation at 12,000 rpm for 45 min at 4°C for removal of the organic solvent and hardening of the NPs. The NPs obtained were suspended in water and again centrifuged (12,000 rpm for 60 min). The process was repeated three times, and finally, the NPs were prefrozen at –80°C overnight then were freeze-dried (Four Ring Fury

Inc, Beijing, China) for 24 h to obtain the powdered form of NPs. Likewise, EGCG-NPs were prepared and stored at 4°C under anhydrous conditions until it was used for further studies (at least 2 months).

Neil Red-NPs were also prepared using an oil-in-water emulsion solvent evaporation technique as previously described. PLGA (10mg) and Neil Red (10 ug) were added to DCM (1 mL) to form the organic phase. ddH₂O was used instead of EGCG as the internal aqueous phase. Other steps are consistent with preparation methods of EGCG-NPs.

Characterization of NPs

Particle Size, Zeta Potential, and Surface Morphology of the NPs

The mean particle size and distribution, as well as the zeta potential of the EGCG-loaded NPs (1 mg/mL in H₂O), were determined using the dynamic light scattering technique with a Zetasizer Nano-ZS (Malvern Instruments, Malvern, UK). Scanning electron microscopy (SEM, Zeiss-Supra 55VP, Germany) was performed to observe the surface morphology of NPs.

Drug Loading and Encapsulation Efficiency

Drug loading and encapsulation efficiency were determined by Ultra Performance Liquid Chromatography (UPLC, MK-II, Waters, Milford, CT, USA). EGCG was quantified by UV detection at 254 nm. Briefly, an accurately weighed sample of drug-loaded NPs (10mg) were suspended in dichloromethane (1mL), and then vortexed vigorously for 5 min. Then centrifuged at 12,000 rpm for 60 minutes. Next, the supernatant was collected and filtered using a 0.45 μm filter. The amount of drug (mg) was calculated from the standard curve drawn for a varying amount of drug (mg) and integrated. Drug loading (DL) and encapsulation efficiency (EE) were determined from the following equation:

$DL = M/M_{np} \times 100\%$, $EE = M/M_{in} \times 100\%$, where M is the actual mass of drug-loaded in the NPs, M_{np} is the total mass of NPs, and M_{in} is the initial mass used in the preparation of NPs.²⁵

In vitro Release of EGCG from PLGA-NPs

EGCG-loaded NPs were evaluated for their in vitro release kinetics using the dialysis method for 14 days. A weighed amount of EGCG-NPs (10 mg) was dispersed in 1 mL phosphate-buffered saline (PBS; pH 7.4), after which the solution was transferred to a dialysis bag (molecular weight cut-off 12 kDa) and allowed to dialyze against 200 mL of the same buffer at 37°C±0.5°C, with stirring at 100 rpm in a shaking incubator (Unimax 1010, Heidolph, Schwabach, Germany).

Sampling was performed at specified time intervals, and an equal amount of fresh PBS was added. Each drug release experiment was tested in triplicate in vitro. Next, the content of EGCG in PBS was determined by UPLC analysis.

Cytotoxicity Study

H1299 and A549 cells were plated at 3×10^3 per well in 100 μL of complete culture medium in 96 well plate. Cells (60% confluent) were treated with free EGCG and EGCG-NPs with the indicated doses (3.125–25 μM). 72- or 96-hour post-treatment the medium was removed and cells were washed with PBS and incubated for 10 μL CCK8. The absorbance was recorded at 450 nm on a microplate reader. Experiments were repeated three times with similar results. The effect of each treatment was assessed as a percentage of cell viability in which the untreated control was taken as 100% viable.²⁶

Annexin V-FITC/PI Double Staining

A549 and H1299 cells were seeded in 6-well plates (5×10^5 cells/mL) and exposed to EGCG or EGCG-NPs for 96 h. Then, the cells were stained using the Annexin V-FITC/PI double-fluorescence apoptosis detection kit (BD Pharmingen, #9,057,689) in accordance with the manufacturer's guidelines. The samples were analyzed using a flow cytometer (FACSCalibur, BD Biosciences) within 1 h of staining. Data analysis was performed using the FlowJo software package.

Cellular Uptake of the NPs

A549 and H1299 cells were incubated with Neil red-loaded NPs (red) and free Neil red for 4 h, respectively. Cells were harvested 4 h after incubation with NPs containing fluorescent-PLGA (red). Next, the nucleus was stained with DAPI (blue) and the cells were fixed with 4% paraformaldehyde at room temperature. The inverted fluorescence microscope (Thermo Fisher Scientific Inc, Waltham, MA, USA) was used to observe the cellular uptake. Neil red (NR), an organic fluorescent dye, was used to demonstrate the uptake of NPs in tumor cells.

Bio-Layer Interferometry (BLI) Kinetic Binding Studies

EGCG-NF-κB kinetic studies were conducted using the Octet Red 96 instrument (FortéBio, Silicon Valley, California, USA). The purified NF-κB protein (99% purity) (Shengzhe Biological Technology Inc, Hainan, China) was loaded onto

Streptavidin biosensors (FortéBio, Silicon Valley, California, USA) at 1000 rpm for 600 s, and the baseline was stabilized for 60 s. EGCG was diluted to the final concentrations of 100 μM , 50 μM , 25 μM , 12.5 μM , and 6.125 μM in PBS with Tween[®], respectively, and associated with the protein on the loaded sensors at 1000 rpm for 60 s, and dissociated for 60 s. The dissociation constants (KD) were analyzed with FortéBio Octet Data Analysis Software version 9.0.0.14.

Quantitative Real-Time PCR (qRT-PCR)

A549 and H1299 cells were treated with free-EGCG (12.5, 25 μM) and EGCG-NPs (12.5, 25 μM) for 48 h. Total RNA was extracted from lung cancer cells using the TRIzol reagent (Invitrogen, USA) and cDNA was synthesized with the PrimeScript RT Reagent Kit (TaKaRa #RR047A). qPCR was performed on the LightCycler 96 Real-Time PCR system (Roche, G10120-100G, Switzerland) with SYBR Premix Ex Taq (TaKaRa #RR420A). Relative expression was normalized to that of GAPDH by the $2^{-\Delta\Delta\text{Ct}}$ method. Analysis of each gene was performed at least three times. The sequences of all primers used for the qRT-PCR analysis are listed in Table 1.

In vivo Studies in the Patient-Derived Xenograft (PDX) Model

This study was approved by the Institutional Review Board of Fujian Medical University (Approval Number:

FJMU-IACUC-18-107), and written informed consent was obtained from each participant. The study was carried out in accordance with the guidelines for the care and use of human specimens and animals, including in the approved protocol. A portion of the patient's resected tumor was immediately placed in Dulbecco's Modified Eagle Medium (DMEM) in ice. Next, 2–3 mm³ tumor portions were implanted on the flanks of male NOD/SCID mice, aged 8–10 weeks. Furthermore, the tumors were implanted into additional Balb/c athymic nude mice when a size of about 1000 mm³ was obtained. The mice were randomly divided into 3 different treatment groups (8 mice per group). PDX tumor bearing mice were treated with PBS (control), free EGCG (10 mg/kg), EGCG-NPs (5 mg/kg) by intraperitoneal injection (i.p.) daily for a month. Tumor volumes were calculated using the following equation: Volume = width \times length²/2.

Histological Examination

Paraformaldehyde-fixed and paraffin-embedded tumor sections were stained with hematoxylin (Service bio #G1004), Ki67 (1:500 dilution, Abcam #AB15580) and phosphorylated NF- κB p65 (1:250 dilution, 3033s, Cell Signaling Technology, USA) using routine methods. TUNEL staining was assessed using the TUNEL Kit (11,684,817,910, Roche, Germany) in accordance with the manufacturer's

Table 1 Primer Sequences of Relevant Genes Used for qRT-PCR

Genes	Accession #	Sequences of Primers
GAPDH	NM-002046.7	Forward: 5'-AAGGTGAAGGTCGGAGTCAAC-3' Reverse: 5'-GGGGTCATTGATGGCAACAATA-3'
BCL2	NM-000657.2	Forward: 5'-GACTTCGCCGAGATGTCCAG-3' Reverse: 5'-GAACTCAAAGAAGGCCACAATC-3'
BCL-XL	NM-138578.3	Forward: 5'-CCCAGAAAGGATACAGCTGG-3' Reverse: 5'-GCGATCCGACTACCAATAC-3'
COX-2	NM-000963.4	Forward: 5'-GATTGACAGCCCACCAACTT -3' Reverse: 5'-CTCTCCACCGATGACCTGAT-3'
TNF α	NM-000594.4	Forward: 5'-CAGAGGGAAGAGTCCCCAG-3' Reverse: 5'-CCTTGGTCTGGTAGGAGACG-3'
Cyclin D1	NM-053056.2	Forward: 5'- CTGGCCATGAACTACCTGGA-3' Reverse: 5'-GTCACACTTGATCACTCTGG-3'
C-MYC	NM-00246.7	Forward: 5'-CCAGCAGCGACTCTAAGG-3' Reverse: 5'-CCAAGACGTTGTGTGTC-3'
TWIST1	NM-000474.4	Forward: 5'-CCATGTCCGCGTCCCACTA-3' Reverse: 5'-CCCACGCCCTGTTTCTTTCTTTGAAT-3'

instructions. The stained slides were digitized using a digital microscope camera (Pannoramic MIDI, 3D HISTECH, Hungary) with a 40× objective. The proportion of cells exhibiting nuclear phospho-NF-κB staining and Ki67-positivity was determined using the ScanScope default nuclear algorithm.

Western Blot

A549 and H1299 cells were treated with free-EGCG (12.5, 25 μM) and EGCG-NPs (12.5, 25 μM) for 48 h. They were then lysed in lysis buffer. After lysis, the samples were boiled and protein samples (40 μg) were fractionated in 10% sodium dodecyl sulfate polyacrylamide gel then transferred to a polyvinylidene difluoride membrane (Millipore, USA). After blocked with 10% nonfat milk, membranes were washed with TBST and then incubated with primary antibodies overnight at 4°C. The following primary antibodies were used: anti-NF-κB (Abcam, #ab32536), anti-P-NF-κB (Abcam, #ab86299), as well as goat anti-rabbit (Proteintech #SA10001-2). Finally, visualization of protein bands were performed using an ECL substrate reagent kit (GE Healthcare) on a Gel Doc XR imaging system (Bio-RAD, USA). β-actin (Abcam#ab227387) was used as the internal reference. The gray value of each protein was determined using Quantity One software, followed by statistical analysis.

Statistical Analysis

In case of all statistical analyses, the significance was set at a probability of $P < 0.05$. All results were reported as the means ± standard error (SD). The Student's *t*-test was used to compare two groups of independent samples. One-way ANOVA analysis was used to evaluate the statistical significance of multiple groups.

Result

Characteristics of EGCG-Loaded PLGA-NPs

Recent studies have shown that free EGCG can achieve cancer-preventive effects at considerably high concentrations,^{6,12-14} possibly restricting the clinical applications. To achieve high therapeutic efficacy with lower drug dosage and reduce drug resistance, it is critical to consider other measures to lower the efficiency concentration of EGCG in lung cancer treatment. It is well known that NPs have shown great potential in various biomedical applications. Particles ranging from 10 to 200 nm are considered ideal NPs to promote tumor accumulation.²⁷⁻²⁹ In our study, EGCG was encapsulated into PLGA-NPs using

the oil-in-water emulsion solvent evaporation technique. (Figure 1A) The dynamic light scattering technique revealed that the formulated NPs were 175.8 ± 3.8 nm in size ($n=9$), with an excellent particle size distribution ($PDI=0.096 \pm 0.015$). As expected, the zeta potential of these particles was found to be negative (-13.70 ± 0.87 mV) due to the negatively charged PLGA (Figure 1B). Furthermore, using SEM, the surface morphology of the NPs was revealed as being smoothly spherical (Figure 1C). The drug content and EE of the optimized formulation were $14.2 \pm 0.3\%$ and $(86.0 \pm 1.5)\%$ ($n = 9$), respectively (Figure 1D).

In vitro Release and Stability of EGCG-Loaded NPs

Notably, burst release always occurs in the in vitro drug release of nanoparticles prepared by nanoprecipitation, caused by the adsorption of drugs onto the surface of NPs.³⁰ However, our study showed approximately 85% increase in EGCG release in 12 days from EGCG-loaded NPs. Only 17% of the total EGCG load was released in the first 3 h, suggesting that the NPs demonstrated a sustained release of the EGCG (Figure 2A). Kinetic stability in a biological medium is an essential property for a drug nanocarrier since a possible therapeutic formulation would need to have the same integrity when formulated and when administered several hours later.²⁹ The result demonstrated that the hydrodynamic diameter remained essentially unchanged as the particle size of 175.8 ± 3.8 nm at the end of the experiment was similar to the starting particle size of 190 ± 3.6 nm (Figure 2B). This indicated that the nanoparticle suspensions did not aggregate or undergo gross degradation throughout the 60-day incubation in PBS (pH 7.4) at 4°C. Therefore, EGCG-loaded PLGA-NPs appear to be promising vehicles for drug delivery.

Cellular Uptake of the NPs and EGCG-NPs Decreased Lung Cancer Cell Viability

An inverted fluorescence microscope was used to demonstrate the uptake of NR-loaded NPs by tumor cells. As shown in Figure 3A and B, the free NR failed to enter A549 and H1299 cells, while NR-loaded NPs could effectively enter A549 and H1299 cells through endocytosis. This result demonstrated the advantage of NPs in transporting drugs into cells. To test the biological efficacy of our nanoconjugate system, we first compared the effectiveness of EGCG-NPs with free EGCG on the proliferative ability of A549 and H1299 cells for 72 and 96

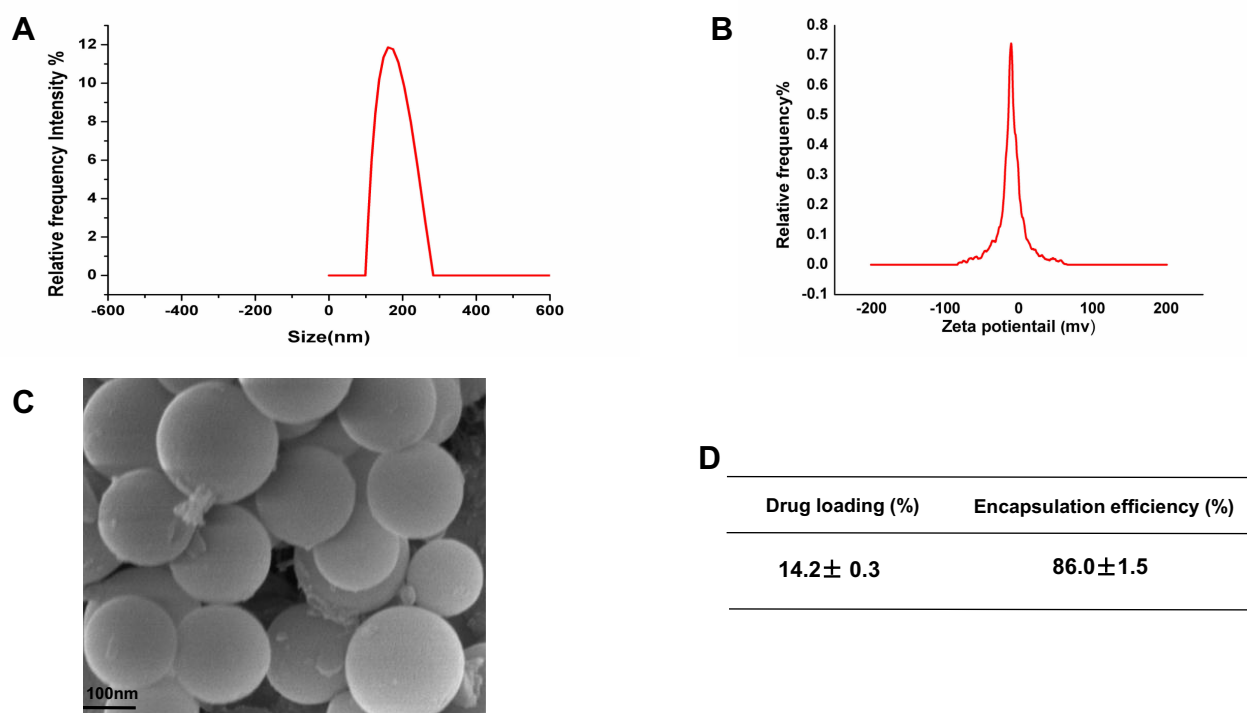


Figure 1 Characterization of EGCG-PLGA-NPs (n=9). **(A)** Particle size distribution based on the images taken. **(B)** Zeta potential of the particles **(C)** Scanning electron microscopy (SEM) images of the NPs. Scale bars = 100 nm. **(D)** Drug loading efficiency and encapsulation efficiency of NPs.

h. Although the safety of PLGA has been widely recognized owing to its biocompatibility and biodegradability, unloaded NPs were also evaluated.²⁵ As shown in [Figure 3](#), the treatment of cells with nanoparticles alone (ddH₂O-NPs) had a negligible effect, confirming the no toxicity property of NPs. However, EGCG-NPs, in comparison to free EGCG, induced a remarkable inhibitory effect on cell growth, with about 3-4-fold superior efficacy. As shown in [Figure 3C](#), in A549, the inhibition ratio of EGCG-NPs was 55% and 65%, while that of native EGCG was around 12.5% and 15%, at 72 h and 96 h, respectively. H1299 cells were also more sensitive to EGCG-NPs than to free EGCG (12.5, 25 μ M) ([Figure 3E](#)). According to previous reports,³¹ drug-loaded nanoparticles can enter tumor cells through endocytosis and then release the drug into cells. This approach could overcome the mechanism of resistance in tumor cells by avoiding the efflux of P-glycoprotein.³¹ Similar effects were observed at 96 h post-treatment, suggesting a sustained release of EGCG from the nanoparticles ([Figure 3D](#) and [F](#)). The IC₅₀ on A549 and H1299 cells also demonstrated that EGCG-NPs significantly enhanced the anti-proliferative effect ([Figure 3G](#)).

Apoptosis-Inducing Potential of EGCG Was Enhanced by EGCG-Loaded PLGA-NPs

Previously, we demonstrated that EGCG reduced the viability of lung cancer cells by inducing apoptosis.⁶ In detail, the percentage of apoptotic A549 (H1299) cells after 48 h of treatment with 80 and 160 μ M of EGCG was found to be 4.5% (5.1%) and 22.2% (33.5%), respectively.⁶ Based on the above results, we determined if the effective concentration of EGCG could be lowered by developing a nanoformulation to induce apoptosis. H1299 and A549 cells were treated with EGCG (12.5, 25 μ M) for 96 h ([Figure 4](#)). Next, the cells were subjected to flow cytometric analysis and the apoptotic cells were detected by Annexin V and PI staining. We observed that the 25 μ M EGCG-NPs induced 72% and 98% apoptosis in A549 and H1299 cells, respectively; however, EGCG only induced 6.3% and 21% apoptosis ([Figure 4A–D](#)) after 96 h of treatment. The data revealed enhanced apoptosis in A549 and H1299 cells treated with EGCG-NPs compared to that observed following treatment with free EGCG.

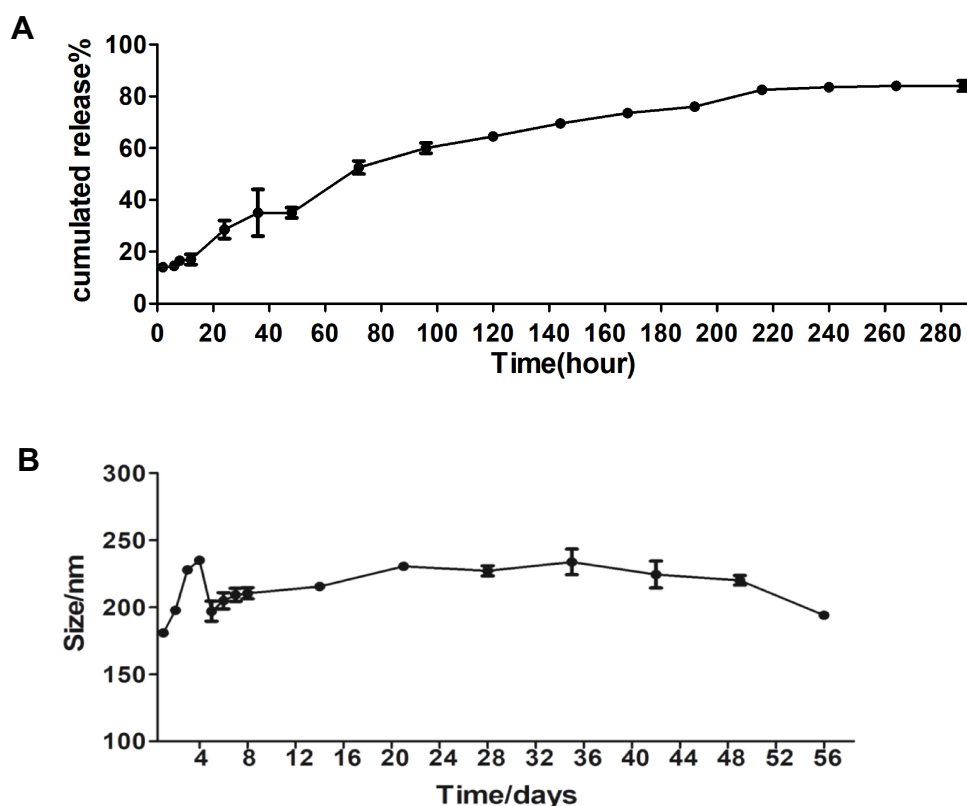


Figure 2 In vitro release and stability of EGCG-NPs. Release profile of (A) from EGCG-NPs (B) stability of EGCG-NPs in PBS at 4°C. The average hydrodynamic diameter (nm) of EGCG-NPs as a function of time (h).

EGCG-Loaded PLGA-NPs Enhanced EGCG-Induced Apoptosis by Suppression of NF-κB

NF-κB is linked to the proliferation of tumor cells and has shown EGCG-induced lung cancer apoptosis via the down-regulation of NF-κB.⁶ In our study, we further examined whether EGCG-NPs induced apoptosis by suppression of NF-κB. First, the binding affinity of EGCG for protein-NF-κB was detected using BLI analysis (Figure 5A). The results demonstrated that binding decreased with increasing EGCG concentration, indicating that EGCG blocked NF-κB activity in a concentration-dependent manner, with $KD=4.8 \times 10^{-5}$ M. (Figure 5A and B).

Next, we investigated whether the cellular cytotoxicity induced by EGCG-NPs in lung cancer cells was also mediated by the same mechanism as previously reported.⁶ The cells were incubated with different concentrations of free EGCG or EGCG-NPs for 48 h. In A549, EGCG-NPs treatment (12.5–25 μM) demonstrated obvious inhibition of phospho-NF-κB protein (Figure 5C and E). Similar results were also reported in the H1299 cell line (Figure 5D and F).

To be sure that EGCG-induced apoptosis is triggered by inhibited NF-κB, we then examined expressions of several NF-κB pathway-related genes that mediate cellular proliferation, invasion, and angiogenesis, including BCL2, BCL-XL, COX-2, TNFα, cyclinD1, C-MYC, TWIST1, and MMP2.^{1,32} The result showed the expression of these genes was partially inhibited by EGCG, dose-dependent significantly inhibition was observed with the EGCG-NPs and was consistent with a decrease in phospho-NF-κB expression (Figure 5G and H).

EGCG-Loaded PLGA-NPs Enhanced Antitumor Potential in vivo

Since EGCG-NPs effectively suppressed the growth of tumor cells in vitro, we examined its efficacy and safety in vivo. We used the human lung cancer PDX mouse model, which has been shown to recapitulate the histologic and genetic features of human primary tumors and is useful in assessing treatment response.³³ We treated PDX model with EGCG-NPs (5 mg/kg i.p.) and free EGCG (10 mg/kg i.p.). We failed to observe any noticeable differences in body weight, suggesting that our nanoformulation or free EGCG did not induce any apparent toxicity in the animals (Figure 6A). The group treated with

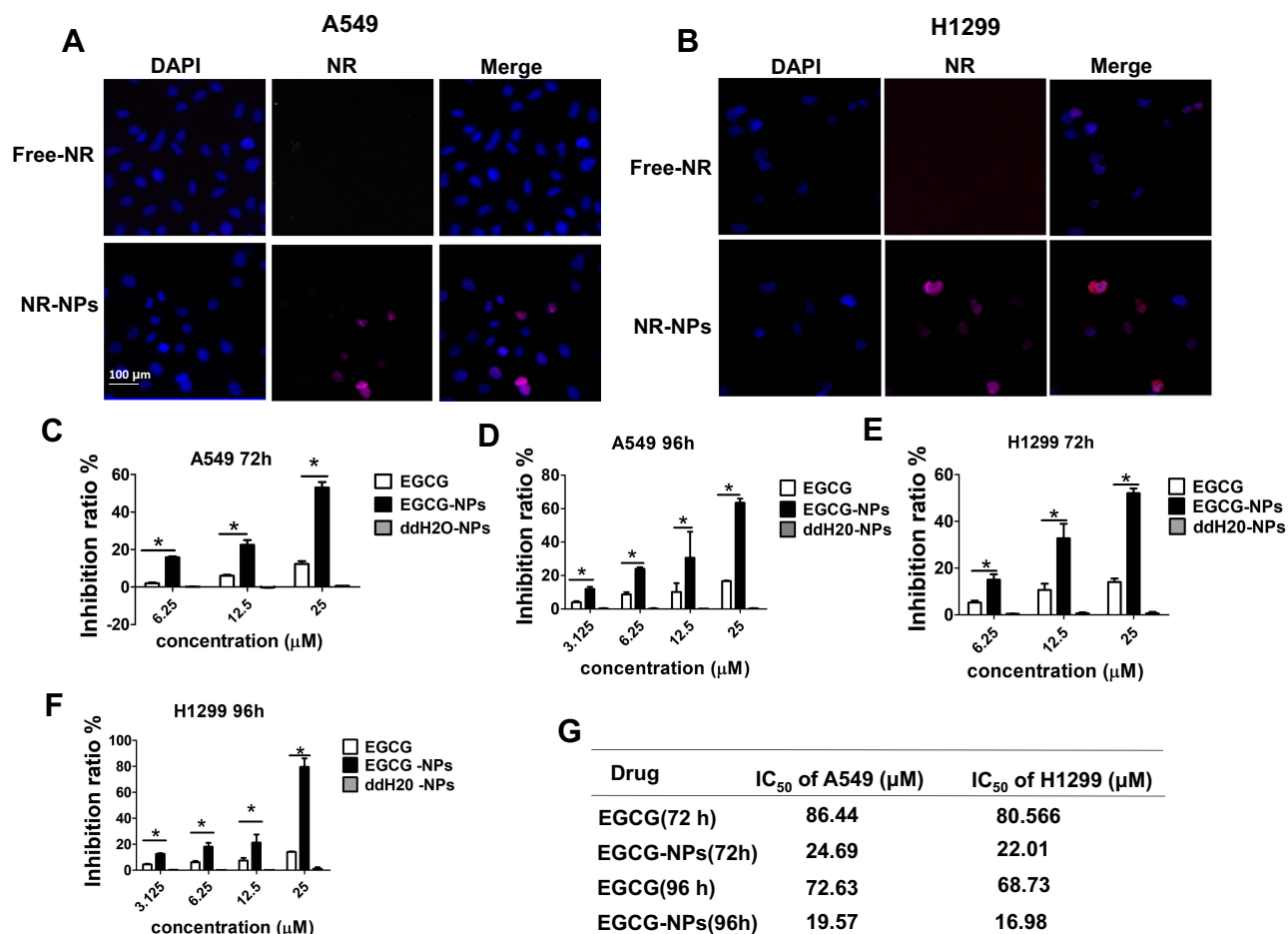


Figure 3 Cellular uptake of the NPs and the effect of EGCG-NPs on lung cancer cell proliferation. Inverted fluorescence microscopy of lung cancer cells harvested 4 h after incubation of NP containing fluorescent-PLGA (red) and counterstained with DAPI for nucleus detection (blue). RGD-NP and non-targeted NP in A549 (A) and H1299 (B). Effects of EGCG-NPs on proliferation of (C, D) A549 cells, (E, F) H1299 cells as determined by CCK8 assay at 72 h and 96 h, respectively. (G) The IC₅₀ on A549 and H1299 cells. Means \pm SDs of three independent experiments are shown. *P < 0.05.

EGCG-NPs indicated a significant decrease in both tumor volume and tumor weight compared to those observed in the control group and the EGCG treatment group (Figure 6B–D). Next, we performed Ki67 and TUNEL assays using the xenograft tumor tissues to measure apoptosis and tumor proliferation. As shown in Figure 6E, EGCG-NPs increased the efficacy of EGCG in pro-apoptosis (number of green color spots in TUNEL increased) and inhibition of proliferation (brown color spots number of Ki67 decreased), similar to our in vitro results. In our last set of experiments, to further elucidate the mechanism underlying the inhibition of tumor growth, we detected the expression of phospho-NF- κ B in the tumor tissues. The results of the immunoblot analysis clearly indicated that EGCG-NPs enhanced the downregulation of phospho-NF- κ B compared to free EGCG. Collectively, PLGA-encapsulated EGCG significantly enhances the chemotherapeutic efficacy of EGCG against lung cancer in vivo.

Discussion

Despite significant efficacy in preclinical settings, green tea has demonstrated limited efficacy in clinical settings, mainly due to poor bioavailability and perceived toxicity.^{34–40} To circumvent such unwanted outcomes while preserving the antitumor activity, we developed an appropriate EGCG-NPs formulation for cancer treatment. In the present study, we prepared EGCG-loaded PLGA-NPs, which demonstrated substantial efficacy in the PDX model, with great potential for further therapeutic advancement in clinical settings.

We prepared EGCG-loaded PLGA-NPs and systematically evaluated the effect of formulation variables such as sonication power, volume ratio between EGCG and PLGA, sonication time and PVA concentration on particle size and EE% (Supplementary Figure 1). The optimal formulations obtained were of submicron size 175.8 ± 3.8 , with an entrapment efficiency of $86.0 \pm 1.5\%$.

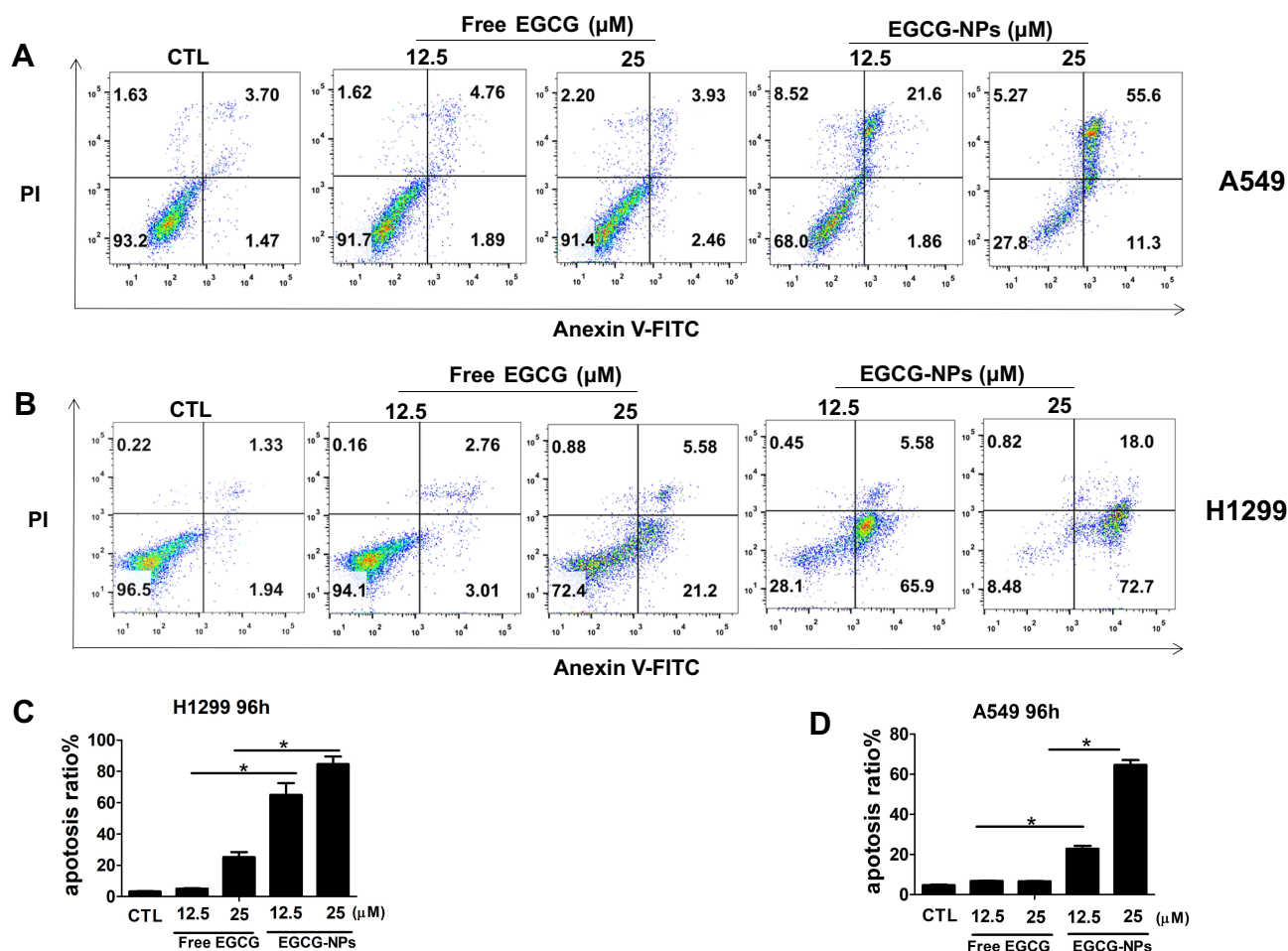


Figure 4 Induction of apoptosis by EGCG-NPs in lung cancer cells. (A, B) Flow cytometry images. (C, D) Quantitative analysis of the percentage of apoptotic cells after 96 h incubation. The percentage of total apoptotic cells was derived from the sum of early and late apoptotic cells. Means \pm SDs of three independent experiments are shown. * $P < 0.05$.

Next, we investigated the inhibitory potential of our PLGA based nanoformulation containing EGCG on cell growth, confirming its several fold dose advantage over native EGCG, the induction of apoptosis, and suppression of phospho-NF- κ B expression. We observed that the NPs showed sustained release and a 3–4-fold greater ability to suppress proliferation of A549 and H1299 cells than free EGCG, possibly due to enhanced drug uptake. Siddiqui et al³⁴ have suggested that enhanced uptake of phytochemicals, when formulated with NPs, correlates with their enhanced antitumor activity.^{23,41}

It is well established that apoptosis is a major mechanism by which various anticancer agents destroy tumor cells.⁴² We observed that EGCG-NPs enhanced apoptosis in lung cancer. Notably, the activation of NF- κ B appears to be a major pathway involved in the proliferation of tumor cells, chemoresistance, and inflammation.^{32,43} Using BLI, we documented the

inhibitory potential of EGCG against NF- κ B ($KD=4.8 \times 10^5$ M). In our present study, we observed that low doses of EGCG-loaded NPs (12.5, 25 μ M) suppressed NF- κ B more efficiently than free EGCG. When examined for its ability to suppress NF- κ B-regulated genes (BCL2, BCL-XL, COX-2, TNF α , cyclinD1, C-MYC, TWIST1, and MMP2), EGCG-NPs were found to be more effective than free EGCG.

The final goal of our study was to examine the in vivo efficacy of our nanoformulation in the lung cancer PDX model. Classical models for cancer drug screening include cultured human tumor cell lines and rodent xenografts comprising of human cells grown subcutaneously in immunodeficient animals. One obvious problem with these models is the artificial nature of tumor cell lines, typically passaged for many generations in enriched culture media. These models may not be generally representative of the genetic and epigenetic heterogeneity of the original primary tumor.⁴⁴

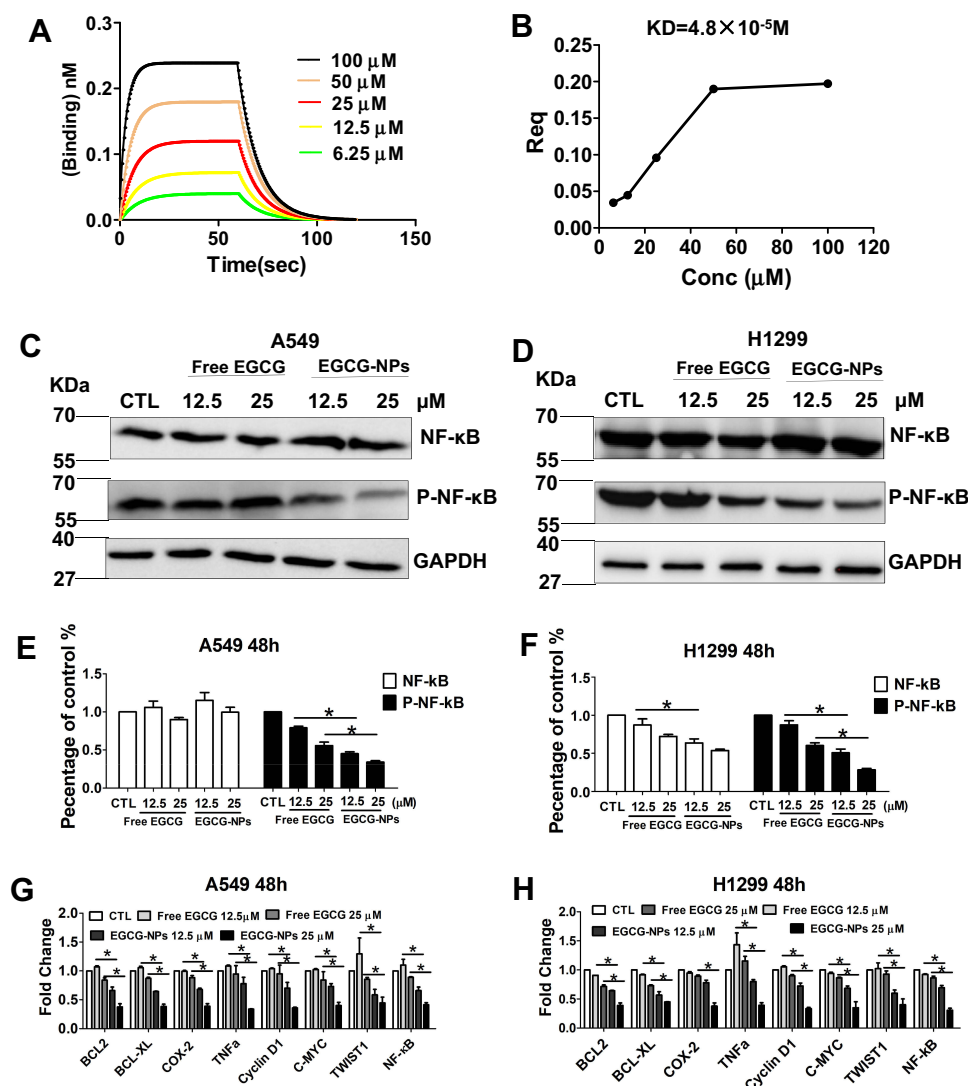


Figure 5 EGCG-NPs induce lung cancer apoptosis via NF- κ B inhibition. **(A, B)** NF- κ B specifically binds to the active form of EGCG by BLI kinetic binding assay. Biotin-labeled NF- κ B was immobilized onto the Streptavidin Biosensors and tested for kinetic binding to various concentrations of EGCG. The dissociation constant of NF- κ B and EGCG is 4.8×10^{-5} M. **(B)** Steady-state analysis, $R^2=1$. **(C–F)** Western blot analysis of total NF- κ B and phosphorylated NF- κ B p65 in A549 and H1299 whole-cell lysates after treatment with EGCG and EGCG-NPs (12.5 μ M and 25 μ M) for 48 h. **(G, H)** qRT-PCR analysis of C-MYC, Cyclin D1, Bcl-2, Bcl-xL, COX-2, TNF- α , TWIST1, and MMP2 after treatment with EGCG and EGCG-NPs (12.5 μ M and 25 μ M) for 48 h. Data are shown as the mean \pm SDs. (n=3). * P < 0.05.

However, the PDX mouse model, as a novel preclinical cancer model, was highly relevant to real human tumor growth, and the tumors maintained the original molecular characteristic and heterogeneity.⁴⁵ Thus, our results indicate considerable credibility for translating this knowledge from the bench to bedside.

In the lung cancer PDX model, tumor formation in mice treated with EGCG and EGCG-NPs was delayed significantly compared to that in the control group mice. As shown in **Figure 6D**, in the untreated control mice group, the targeted tumor volume (2000 mm³) was reached within 30 days. At this point, the calculated volume in the EGCG treated group was

1700 mm³, while in the nano-EGCG treated group the tumor volume was approximately 1200 mm³, despite the use of a 2-fold higher dose of the native compound. Additionally, the EGCG-NPs (5 mg/kg) indicated a dosage advantage compared to that observed in the G Jin's study, where PDX tumor-bearing mice were treated with 50 mg/kg free EGCG daily.⁴⁵ We further evaluated the induction of apoptosis and inhibition of tumors isolated from the animals to define the mechanism underlying tumor growth inhibition. We observed the expression of Ki67 (key cell proliferation markers) and, as expected, Ki67 was abundant in the nuclei of the untreated control. Furthermore, treatment with free EGCG inhibited the

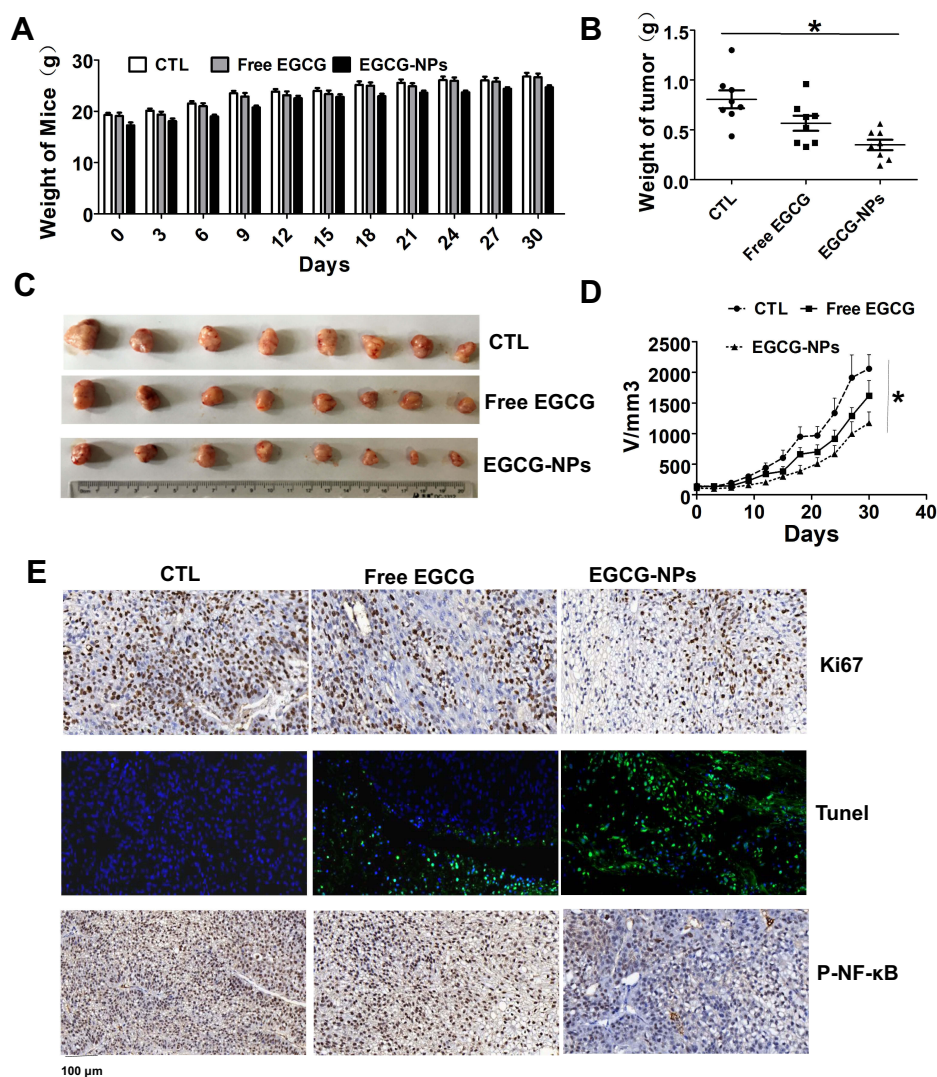


Figure 6 Comparative effects of EGCG-NPs (5 mg/kg) and free EGCG (10 mg/kg) on tumor growth in a PDX model. **(A)** No significant body weight loss is observed during the treatment period in mice. **(B)** Treatment with EGCG-NPs resulted in a significant decrease in tumor weight. **(C)** Representative images of tumors from each group at the termination of the experiment. **(D)** Graph showing the tumor volumes in each group, assessed using caliper measurements. Data are expressed as the mean \pm SDs, $n=8$. **(E)** Immunohistochemistry staining (Ki67, TUNEL, and phospho-NF- κ B) of tumor tissues. * $P < 0.05$.

expression level to a certain extent. Notably, EGCG-NPs significantly inhibited the Ki67. The TUNEL assay, further clarified that the EGCG-NPs could enhance the induction of apoptosis. Lastly, the expression of phospho-NF- κ B in the tumor was significantly inhibited by EGCG-NPs. In this respect, it is convinced to consider that the increased killing of tumor cells by EGCG-NPs might occur in the same manner as in the PDX model. The increased accumulation of EGCG-NPs in defective, leaky, and highly permeable vascular tumor tissue, possibly due to the enhanced permeability and retention effect,^{46,47} allowed nanosized anticancer compounds to act more effectively and with reduced side effects of green tea.

Although in the present study, we developed PLGA-NPs as a delivery system showed that they could enhance the antitumor effect. However, the formulated delivery system was not able to distinguish among different cells. Drug targeting can improve the efficacy of therapy and reduce side effects associated with drugs.^{48,49} For this purpose, we are planning to attach mAb on the nanoparticle surface via the adsorption process.⁵⁰ The goal would be to give the modified nanoparticle delivery systems the ability to recognize and target lung cancer cell and offers the potential as a much more effective antitumor therapy.

Conclusion

Collectively, the present study showed that our nanoformulation of EGCG was effective in both in vitro and in vivo animal model systems of lung cancer. This clearly indicates that by using this formulation strategy, green tea polyphenols could be delivered in physiologically active concentrations. Thus, the outcome of this study could have direct practical implication, with translational relevance in human lung cancer patients.

Abbreviations

EGCG, (-)-epigallocatechin gallate; PLGA, poly(lactic-co-glycolic acid); SD, standard deviation; NPs, nanoparticles; NR, Nile Red; EE, encapsulation efficiency; DL, drug loading; PDX, patient-derived tumor xenograft; SEM, scanning electron microscope; NSCLC, non-small cell lung cancer; UPLC, ultra-performance liquid chromatography; CCK8, Cell Counting Kit-8; DCM, dichloromethane.

Acknowledgments

This work was supported by the National Natural Sciences Foundation of China (grant number 81572286, 81872186); Joint Funds for the innovation of science and technology, Fujian Province (grant number 2017Y9065); Scientific research funding of School and Hospital of Stomatology, Fujian Medical University (grant number 2018KQYJ01), and the Sailing project of Fujian Medical University (2017XQ2020). We thank Dr. April Darling (University of Pennsylvania School of Medicine) and Ms Qingling Li (Fujian Medical University School of Stomatology) for the language editing during the revising of the manuscript.

Disclosure

The authors report no conflicts of interest in this study.

References

- Bremnes RM, Busund L-T, Kilvaer TL, et al. The role of tumor-infiltrating lymphocytes in development, progression, and prognosis of non-small cell lung cancer. *J Thorac Oncol*. 2016;11(6):789–800. doi:10.1016/j.jtho.2016.01.015
- Castellanos-Rizaldos E, Grimm DG, Tadigotla V, et al. Exosome-based detection of EGFR T790M in plasma from non-small cell lung cancer patients. *Clin Cancer Res*. 2018;24(12):2944–2950. doi:10.1158/1078-0432.CCR-17-3369
- Hu SY, Huang KM, Adams EJ, Loprinzi CL, Lustberg MB. Recent developments of novel pharmacologic therapeutics for prevention of chemotherapy-induced peripheral neuropathy. *Clin Cancer Res*. 2019;25(21):6295–6301. doi:10.1158/1078-0432.CCR-18-2152
- Shankar S, Ganapathy S, Srivastava RK. Green tea polyphenols: biology and therapeutic implications in cancer. *Front Biosci*. 2007;12:4881–4899. doi:10.2741/2435
- Yang CS, Wang X, Lu G, Picinich SC. Cancer prevention by tea: animal studies, molecular mechanisms and human relevance. *Nat Rev Cancer*. 2009;9(6):429–439. doi:10.1038/nrc2641
- Zhang LZ, Xie J, Gan RH, et al. Synergistic inhibition of lung cancer cells by EGCG and NF- κ B inhibitor BAY11-7082. *J Cancer*. 2019;10(26):6543–6556. doi:10.7150/jca.34285
- Bailey HH, Mukhtar H, Almoustafa HA, Alshawsh MA, Chik Z. Green tea polyphenols and cancer chemoprevention of genitourinary cancer. *Am Soc Clin Oncol Educ Book*. 2014;287:92–96. doi:10.1200/EdBook_AM.2013.33.92
- Khan N, Mukhtar H. Tea and health: studies in humans. *Curr Pharm Des*. 2013;19:6141–6147. doi:10.2174/1381612811319340008
- Siddiqui IA, Tarapore RS, Mukhtar H. Prevention of skin cancer by green tea: past, present and future. *Cancer Biol Ther*. 2009;8:1288–1291. doi:10.4161/cbt.8.13.9022
- Butt MS, Sultan MT. Green tea: nature's defense against malignancies. *Crit Rev Food Sci*. 2009;49:463–473. doi:10.1080/10408390802145310
- Kidd PM. Bioavailability and activity of phytosome complexes from botanical polyphenols: the silymarin, curcumin, green tea, and grape seed extracts. *Altern Med Rev*. 2009;14:226–246.
- Hsieh DS, Wang H, Tan S-W, et al. The treatment of bladder cancer in a mouse model by epigallocatechin-3-gallate-gold nanoparticles. *Biomaterials*. 2011;32(30):7633–7640. doi:10.1016/j.biomaterials.2011.06.073
- Du GJ, Zhang ZY, Wen XD, et al. Epigallocatechin gallate (EGCG) is the most effective cancer chemopreventive polyphenol in green tea. *Nutrients*. 2012;4(11):1679–1691. doi:10.3390/nu4111679
- Luo KW, Chen W, Lung WY, et al. EGCG inhibited bladder cancer SW780 cell proliferation and migration both in vitro and in vivo via down-regulation of NF- κ B and MMP-9. *J Nutr Biochem*. 2017;41:56–64. doi:10.1016/j.jnutbio.2016.12.004
- Nie S, Emory SR. Probing single molecules and single nanoparticles by surface-enhanced raman scattering. *Science*. 1997;275(5303):1102–1106. doi:10.1126/science.275.5303.1102
- Rosi NL, Giljohann DA, Thaxton CS, et al. Oligonucleotide-modified gold nanoparticles for intracellular gene regulation. *Science*. 2006;312(5776):1027–1030. doi:10.1126/science.1125559
- Gref R, Minamitake Y, Peracchia MT, Trubetskov V, Torchilin V, Langer R. Biodegradable long circulating polymeric nanospheres. *Science*. 1994;263:1600–1603. doi:10.1126/science.8128245
- Blakely CM, Pazarentzos E, Krogan NJ, Bivona TG. NF- κ B-activating complex engaged in response to EGFR oncogene inhibition drives tumor cell survival and residual disease in lung cancer. *Cell Rep*. 2015;11:98–110. doi:10.1016/j.celrep.2015.03.012
- Safer AM, Leporatti S, Jose J, Soliman MS. Conjugation of EGCG and chitosan NPs as a novel nano-drug delivery system. *Int J Nanomedicine*. 2019;14:8033–8046. doi:10.2147/IJN.S217898
- Su JQ, Guo Q, Chen YL, Mao L, Gao YX, Yuan F. Utilization of β -lactoglobulin-(-)-epigallocatechin-3-gallate(EGCG) composite colloidal nanoparticles as stabilizers for lutein pickering emulsion. *Food Hyd*. 2020;98:105293. doi:10.1016/j.foodhyd.2019.105293
- Wu SC, Yang XR, Luo FH, et al. Biosynthesis of flower-shaped Au nanoclusters with EGCG and their application for drug delivery. *J Nanobiotechnol*. 2018;90:1575–1590.
- Ringsdorf H. Structure and properties of pharmacologically active polymers. *J Polym Sci Polym Symp*. 1975;51:135–153. doi:10.1002/polc.5070510111
- Danhier F, Ansorena E, Silva JM, Coco R, Le Breton A, Preat V. PLGA-based nanoparticles: an overview of biomedical applications. *J Control Release*. 2012;161:505–522. doi:10.1016/j.jconrel.2012.01.043
- Varypataki EM, Silva AL, Barnier-Quer C, Collin N, Ossendorp F, Jiskoot W. Synthetic long peptide-based vaccine formulations for induction of cell mediated immunity: a comparative study of cationic liposomes and PLGA nanoparticles. *J Control Release*. 2016;226:98–106. doi:10.1016/j.jconrel.2016.02.018

25. Lu B, Lv X, Le Y. Chitosan-modified PLGA nanoparticles for control-released drug delivery. *Polymers*. 2019;11(2):304. doi:10.3390/polym11020304
26. Zou J, Yang Y, Liu XR. Polydatin suppresses proliferation and metastasis of non-small cell lung cancer cells by inhibiting NLRP3 inflammasome activation via NF- κ B pathway. *Biomed Pharmacother*. 2018;108:130–136. doi:10.1016/j.biopha.2018.09.051
27. Fox ME, Szoka FC, Frechet JM. Soluble polymer carriers for the treatment of cancer: the importance of molecular architecture. *Acc Chem Res*. 2009;42:1141–1151. doi:10.1021/ar900035f
28. Kobayashi H, Watanabe R, Choyke PL. Improving conventional enhanced permeability and retention (EPR) effects; what is the appropriate target? *Theranostics*. 2014;4:81–89. doi:10.7150/thno.7193
29. Chen MS, Ouyang HC, Zhou SY, Li JY, Ye YB. PLGA-nanoparticle mediated delivery of anti-OX40 monoclonal antibody enhances anti-tumor cytotoxic T cell responses. *Cell Immunol*. 2014;287:91–99. doi:10.1016/j.cellimm.2014.01.003
30. Almoustafa HA, Alshawsh MA, Chik Z. Technical aspects of preparing PEG-PLGA nanoparticles as carrier for chemotherapeutic agents by nanoprecipitation method. *Int J Pharm*. 2017;533:275–284. doi:10.1016/j.ijpharm.2017.09.054
31. Cartiera MS, Johnson KM, Rajendran V, Caplan MJ, Saltzman WM. The uptake and intracellular fate of PLGA nanoparticles in epithelial cells. *Biomaterials*. 2009;30:2790–2798. doi:10.1016/j.biomaterials.2009.01.057
32. Ngoc TV, Park MA, Shultz MD, Bulut GB, Ladd AC, Chalfant CE. Caspase-9b interacts directly with cIAP1 to drive agonist-independent activation of NF- B and lung tumorigenesis. *Cancer Res*. 2016;76(10):2977–2989. doi:10.1158/0008-5472.CAN-15-2512
33. Chen YC, Zhang R, Wang L, et al. Tumor characteristics associated with engraftment of patient-derived non-small cell lung cancer xenografts in immunocompromised mice. *Cancer*. 2019;125(21):3738–3748. doi:10.1002/cncr.32366
34. Siddiqui IA, Adhami VM, Bharali DJ, et al. Introducing nanochemoprevention as a novel approach for cancer control: proof of principle with green tea polyphenol epigallocatechin-3-gallate. *Cancer Res*. 2009;69:1712–1716. doi:10.1158/0008-5472.CAN-08-3978
35. Khan N, Bharali DJ, Adhami VM, et al. Oral administration of naturally occurring chitosan-based nanoformulated green tea polyphenol EGCG effectively inhibits prostate cancer cell growth in a xenograft model. *Carcinogenesis*. 2014;35:415–423. doi:10.1093/carcin/bgt321
36. Siddiqui IA, Adhami VM, Chamcheu JC, Mukhtar H. Impact of nanotechnology in cancer: emphasis on nanochemoprevention. *Int J Nanomedicine*. 2012;7:591–605. doi:10.2147/IJN.S26026
37. Siddiqui IA, Adhami VM, Ahmad N, Mukhtar H. Nanochemoprevention: sustained release of bioactive food components for cancer prevention. *Nutr Cancer*. 2010;62:883–890. doi:10.1080/01635581.2010.509537
38. Siddiqui IA, Mukhtar H. Nanochemoprevention by bioactive food components: a perspective. *Pharm Res Dordr*. 2010;27:1054–1060. doi:10.1007/s11095-010-0087-9
39. Shanafelt TD, Call TG, Zent CS, et al. Phase 2 trial of daily, oral Polyphenon E in patients with asymptomatic, rai stage 0 to II chronic lymphocytic leukemia. *Cancer*. 2013;119:36370. doi:10.1002/cncr.27719
40. Stingl JC, Etrich T, Muche R, et al. Protocol for minimizing the risk of metachronous adenomas of the colorectum with green tea extract (MIRACLE): a randomised controlled trial of green tea extract versus placebo for nutripvention of metachronous colon adenomas in the elderly population. *BMC Cancer*. 2011;11:360. doi:10.1186/1471-2407-11-360
41. Hillaireau H, Couvreur P. Nanocarriers' entry into the cell: relevance to drug delivery. *Cell Mol Life Sci*. 2009;66:2873–2896. doi:10.1007/s00018-009-0053-z
42. Singhal S, Vachani A, Ozerkis AD, et al. Prognostic implications of cell cycle, apoptosis, and angiogenesis biomarkers in non-small cell lung cancer: a review. *Clin Cancer Res*. 2005;11:3974–3986. doi:10.1158/1078-0432.CCR-04-2661
43. Pires BR, Silva RCM, Ferreira GM, Abdelhay E. NF-kappaB: two sides of the same coin. *Genes*. 2018;9:24. doi:10.3390/genes9010024
44. Zheng DL. Orthotopic tumours, a hot topic for xenograft models? *EBioMedicine*. 2019;41:11–12. doi:10.1016/j.ebiom.2019.02.052
45. Jin G, Yang Y, Liu K, et al. Combination curcumin and (–)-epigallocatechin-3-gallate inhibits colorectal carcinoma microenvironment-induced angiogenesis by JAK/STAT3/IL-8 pathway. *Oncogenesis*. 2017;6:1–12. doi:10.1038/oncsis.2017.84
46. Banerjee SS, Aher N, Patil R, Khandare J. Poly (ethylene glycol) prodrug conjugates: concept, design, and applications. *J Drug Deliv*. 2012;2012:103973. doi:10.1155/2012/103973
47. Yoo JW, Doshi N, Mitragotri S. Adaptive micro and nanoparticles: temporal control over carrier properties to facilitate drug delivery. *Adv Drug Deliv Rev*. 2011;63:1247–1256. doi:10.1016/j.addr.2011.05.004
48. Fahmy TM, Fong PM, Goyal A, Saltzman WM. Targeted for drug delivery. *Mater Today*. 2005;8:18–26. doi:10.1016/S1369-7021(05)71033-6
49. Stella B, Arpicco S, Peracchia MT, et al. Synthesis and multidisciplinary characterization of polyelectrolyte multilayer-coated nano-gold with improved stability toward aggregation. *Colloid Polym Sci*. 2011;289:269–280. doi:10.1007/s00396-010-2343-2
50. Kocbek P, Obermajer N, Cegnar M, Kos J, Kristl J. Targeting cancer cells using PLGA nanoparticles surface modified with monoclonal antibody. *J Control Release*. 2007;120:18–26. doi:10.1016/j.jconrel.2007.03.012

International Journal of Nanomedicine

Publish your work in this journal

The International Journal of Nanomedicine is an international, peer-reviewed journal focusing on the application of nanotechnology in diagnostics, therapeutics, and drug delivery systems throughout the biomedical field. This journal is indexed on PubMed Central, MedLine, CAS, SciSearch®, Current Contents®/Clinical Medicine,

Submit your manuscript here: <https://www.dovepress.com/international-journal-of-nanomedicine-journal>

Dovepress

Journal Citation Reports/Science Edition, EMBase, Scopus and the Elsevier Bibliographic databases. The manuscript management system is completely online and includes a very quick and fair peer-review system, which is all easy to use. Visit <http://www.dovepress.com/testimonials.php> to read real quotes from published authors.